NEARSHORE WAVE DYNAMICS SIMULATED BY BOUSSINESQ TYPE MODELS

Ole R. Sørensen[1], Per A. Madsen[1], and Hemming A. Schäffer[1]

Abstract

This paper presents a numerical study of nearshore wave dynamics including the surf zone. Two different time-domain Boussinesq type formulations are applied for this purpose. The first model incoporates Padé [2,2] dispersion characteristics and lowest order nonlinearity. The second and more sophisticated model incorporates Padé [4,4] characteristics and higher-order nonlinearity in the dispersive terms. The models are validated on the shoaling and breaking of regular and irregular waves with and without an ambient current.

1. INTRODUCTION

Numerical models of nearshore wave hydrodynamics have developed rapidly in complexity over the last decade. Today, the most advanced Boussinesq type models offer an accurate representation of complicated processes such as triad wave interactions and wave-current interaction, while wave breaking of irregular waves and the resulting dissipation processes can be approximated by fairly simple but reasonably accurate descriptions. This allows for a study of a variety of complicated phenomena in the surf zone and in the swash zone.

In previous publications (e.g. Schäffer et al., 1993; Madsen et al., 1997a,b; Sørensen et al., 1998) we have studied and modelled surf zone dynamics such as the shoaling, breaking and runup of regular and irregular waves, the generation and release of low frequency waves, wave-induced rip-currents and circulation cells behind detached breakwaters. For this purpose we have until recently applied a time-domain Boussinesq model (I) in terms of the depth-integrated velocity and including lowest order nonlinearity and Padé [2,2] dispersion characteristics. The results obtained with this model have been satisfactory with a few exceptions. However, it has been clear for some time that this model underestimates the nonlinear shoaling

[1]International Research Centre for Computational Hydrodynamics (ICCH), Danish Hydraulic Institute, Agern Allé 5, DK-2970, Hørsholm, Denmark

near the break point. This shortcoming shows up in the wave height or wave crest variations and even more clearly in the evolution of nonlinear measures such as the skewness and asymmetry.

In this work we introduce a more sophisticated Boussinesq model (II) which includes higher-order nonlinearity in the dispersive terms as well as more accurate linear dispersion characteristics (Padé [4,4]-type). Both models (I and II) are applied in this study to investigate shoaling and breaking of regular and irregular waves on different bathymetries. The emphasis is on the evolution of higher-order statistics in terms of the skewness and asymmetry. Comparisons with physical experiments are presented for three cases. The effect of an opposing current on the shoaling and breaking of regular waves on a sloping plane beach is also investigated. Here we concentrate on validating the ability of the breaking model to predict the breaker depth and breaker height.

2. MODEL DESCRIPTION

The two different time-domain Boussinesq formulations considered in this work are described below. For simplicity we shall list the equations for a constant depth althrough the variable-depth terms were included in all computations. Both models are extended into the surf zone by the use of the so-called roller concept as summarized in Section 2.2.

2.1 Boussinesq formulations

Model I is formulated in terms of the depth-integrated horizontal velocity and it retains terms of order $O(\mu^2,\epsilon)$, where ϵ is a measure of the nonlinearity and μ is a measure of linear dispersion. The general two-dimensional equations valid on a sloping bottom were originally derived by Madsen & Sørensen (1992) and later extended to the surf zone by Madsen et al. (1997a,b). In one dimension and on a constant depth the equations read

$$\frac{\partial \eta}{\partial t} + \frac{\partial Q}{\partial x} = 0 \tag{1a}$$

$$Q_t + \epsilon \frac{\partial}{\partial x}\left(\frac{Q^2}{h+\epsilon\eta}\right) + \epsilon R_x + (h+\epsilon\eta)\eta_x + \mu^2\left(\left(v_1 - \frac{1}{3}\right)h^2 Q_{xxt} + v_1 h^3 \eta_{xxx}\right) = O(\epsilon\mu^2, \mu^4) \tag{1b}$$

where Q is the depth integrated velocity, h is the still water depth, η is the surface elevation and v_1=-1/15. This formulation is superior to the classical Boussinesq equations as it incorporates Padé [2,2] dispersion characteristics for pure waves, i.e. in the absence of current. We note that the R-term in (1b) represents the roller dynamics as described in Section 2.2.

Model II is formulated in terms of the horizontal velocity at a certain z/h-location and it retains terms of order $O(\mu^2,\epsilon^3\mu^2)$. The general two-dimensional equations valid on a sloping bottom can be found in Madsen & Schäffer (1998a), and they have previously been solved in one-dimension by Madsen et al. (1996). In one dimension and on a constant depth the equations read

$$\eta_t + h\acute{u}_x + \mu^2\left(\left(\alpha+\frac{1}{3}-\beta_1\right)h^3\acute{u}_{xxx} - \beta_1 h^2\eta_{xxt}\right) + \epsilon(\eta\acute{u})_x +$$

$$\epsilon\mu^2 h^2\frac{\partial}{\partial x}\left(\alpha\eta\acute{u}_{xx} - \beta_1(\eta\acute{u})_{xx}\right) - \epsilon^2\mu^2\frac{h}{2}\frac{\partial}{\partial x}\left(\eta^2\acute{u}_{xx}\right) - \tag{2a}$$

$$\epsilon^3\mu^2\frac{\partial}{\partial x}\left(\frac{1}{6}\eta^3\acute{u}_{xx}\right) = O(\mu^4)$$

$$\acute{u}_t + \eta_x + \mu^2\left((\alpha-\alpha_1)h^2\acute{u}_{xxt} - \alpha_1 h^2\eta_{xxx}\right) + \epsilon\left(\acute{u}\acute{u}_x + \frac{R_x}{h+\epsilon\eta}\right) +$$

$$\epsilon\mu^2\frac{\partial}{\partial x}\left(\alpha h^2\acute{u}\acute{u}_{xx} - \frac{\alpha_1}{2}h^2(\acute{u}^2)_{xx} + \frac{1}{2}h^2(\acute{u}_x)^2 - h\eta\acute{u}_{xt}\right) +$$

$$\epsilon^2\mu^2\frac{\partial}{\partial x}\left(-\frac{1}{2}\eta^2\acute{u}_{xt} + h\eta\left(\acute{u}_x^2 - \acute{u}\acute{u}_{xx}\right)\right) + \tag{2b}$$

$$\epsilon^3\mu^2\frac{\partial}{\partial x}\left(-\frac{1}{2}\eta^2\acute{u}\acute{u}_{xx} + \frac{1}{2}(\eta\acute{u}_x)^2\right) = O(\mu^4)$$

where ú is the velocity in a specific z/h-location and

$$(\alpha,\beta_1,\alpha_1) = \left(\frac{-3-\sqrt{23/35}-2\sqrt{19/7}}{18}\ ,\ \frac{28-2\sqrt{133}}{126}\ ,\ \frac{105-3\sqrt{805}}{1890}\right) \tag{3}$$

Again the R-term in (2b) represents the roller dynamics as described in Section 2.2. Madsen & Schäffer (1998a,b) demonstrated that (2a-b) is Galilean invariant and that it incorporates Padé [4,4] dispersion characteristics for pure waves as well as for waves in currents. Furthermore, the characteristics for shoaling and wave-wave interaction are generally superior to the ones obtained by Model I.

Fig. 1 shows the accuracy of the second order transfer functions derived from the two different Boussinesq formulations. The individual transfer functions are scaled with the target solution of Stokes. We notice that Model II obviously contains the best nonlinear performance, while Model I significantly underestimates the transfer function for larger kh-values.

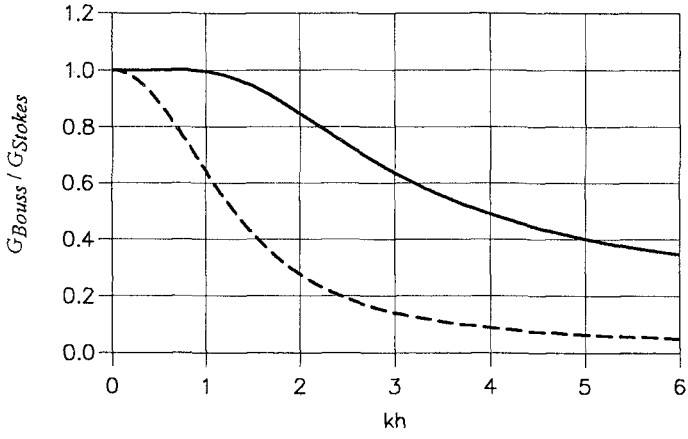

Figure 1 Transfer function for the second harmonic as function of kh for the two Boussinesq-type models. Results scaled by Stokes solution. (- - -) Model I and (——) Model II.

2.2 Breaker model based on the roller concept

Wave breaking is introduced in the Boussinesq equations on the basis of the surface roller concept for spilling breakers as described by Schäffer et al. (1993) and Madsen et al. (1997a, 1997b). The basic principle is that the surface roller is considered as a volume of water carried by the wave with the wave celerity. The influence of breaking on the governing equations is modelled by an additional momentum term orginating from a non-uniform velocity profile due to the presence of the roller. This momentum term can be expressed as

$$R = \frac{\delta}{1 - \delta/d}(c - u) \tag{4}$$

Here d is the total water depth, δ is the roller thickness, c is the roller celerity, while u is the depth-averaged velocity (Q/d) in eq. (1b) and the velocity at a specific z/h-location in eq. (2b).

The instantaneous roller thickness at each point is determined based on a heuristic geometrical approach. Incipent breaking is assumed to occur when the local slope of the surface elevation exceeds an initial critical value, $\tan\phi_B$. During the

transition from initial breaking to a bore-like stage in the inner surf zone the critical angle is assumed to gradually change from ϕ_B to a smaller terminal angle ϕ_0. Hence the instantaneous value of ϕ defining the toe of the roller depends on the age of the roller and is assumed to follow an exponential time-variation with a half time $t_{1/2}$. Locally, the roller is defined as the water above the tangent of slope tanϕ. Prior to inclusion in the governing equations the roller thickness is multiplied by a shape factor. In Model I a constant factor of 1.5 is applied, while a shape factor which has a linear variation from 2 at the toe of the roller to zero at the back of the roller is applied in Model II. The latter modification of the shape factor was introduced because the previous formulation had a tendency to give small spurious oscillations near the back of the roller, when applied to the peaked wave profiles appearing with Model II.

For Model I all test cases in the present paper are modelled with a default set of breaking parameters (ϕ_B, ϕ_0, $t_{1/2}$) = (20 deg, 10 deg, T/5), where T is a characteristic wave period. These parameters were given by Madsen et al. (1997a). However, the calibration of ϕ_B and to some extent $t_{1/2}$ is related to the accuracy of the computed surface elevation before the breaking occurs. As Model II incorporates more nonlinearity, the wave profiles computed by this model will generally contain a higher level of skewness and this will show up in particular near the breaking point. Therefore, the breaking parameters, which have been calibrated on the basis of Model I, have to be revised. In the present paper all simulations with Model II are performed with (ϕ_B, ϕ_0, $t_{1/2}$) = (32 deg, 10 deg, T/10).

The wave celerity, which is an important part of (4), is determined interactively from the instantaneous wave field using

$$c = -\frac{\eta_t}{\eta_x} \tag{5}$$

determined at the steepest point of each wave front.

3. Shoaling and breaking of regular and irregular waves

3.1 Regular waves on a plane sloping beach

Ting and Kirby (1994) presented measurements for spilling breakers on a plane sloping beach with a slope of 1/35 starting in a depth of 0.40 m. As input they generated regular waves with a wave period of 2.0 s and a wave height of 0.125 m. Fig. 2 shows the spatial variation of the crest and trough elevations and of the mean water level computed by the two different Boussinesq models. It is obvious that model II, which contains higher-order nonlinear terms, significantly improves the nonlinear shoaling up to the vicinity of the breaking point. This result is in accordance with the analysis from Fig. 1. The difference between the two model results is emphasized in Fig. 3, which shows the spatial variation of the skewness and asymmetry, and in Fig 4, which shows the computed wave profiles at the point of wave breaking. Again model II is seen to predict a much higher level of nonlinearity.

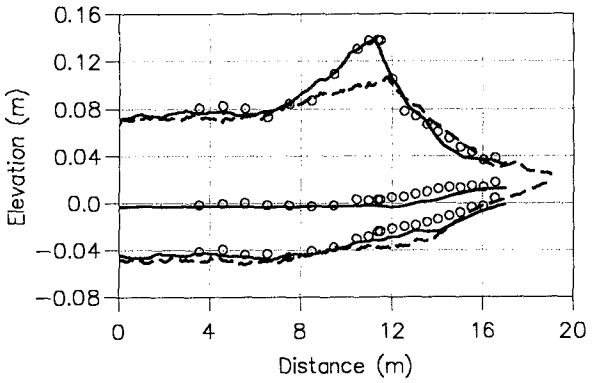

Figure 2 Spatial variation of wave crest elevation, wave trough elevation and mean water level for the test of Ting and Kirby (1994). (- - -) Model I; (——) Model II; (o) experimental data.

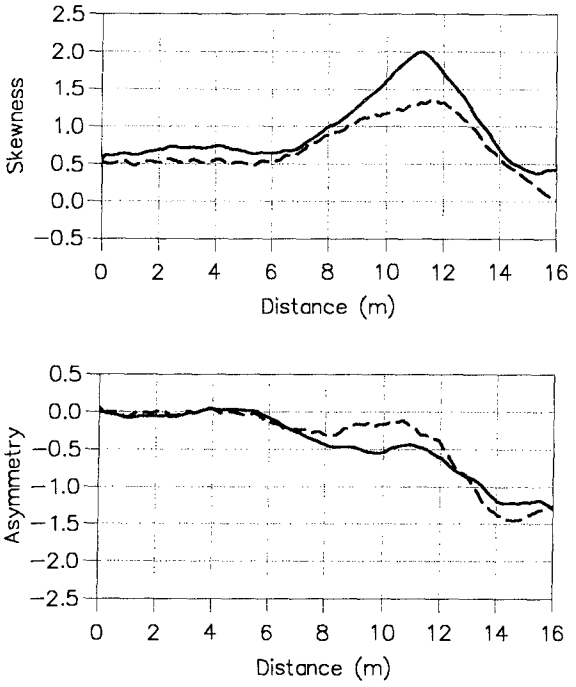

Figure 3 Spatial variation of the skewness and asymmetry for the test of Ting and Kirby (1994), (- - -) Model I and (——) Model II.

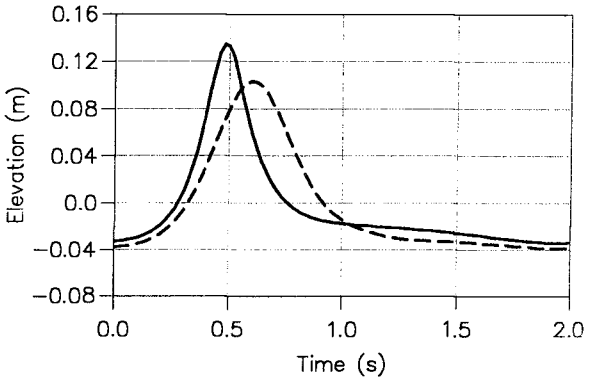

Figure 4 Timeseries of surface elevations at a location near the break point (x=11 m). (- - -) Model I and (——) Model II.

3.2 Irregular waves on a plane sloping beach

This test case is based on the laboratory measurements reported by Cox et al. (1991). Fig. 5 illustrates the experimental setup. The flume consists of a 10 m horizontal section with a water depth of 0.47 m and a 12 m section with a constant slope of 1/20. Measurements of the surface elevation are available at eleven locations (denoted WG1 to WG11) in still water depths of 47, 35, 30, 25, 20, 17.5, 15, 12.5, 10, 7.5 and 5 cm. The input waves are generated on the basis of a target spectrum of Pierson-Moskowitz type with a peak frequency of 1.0 Hz and a significant wave height of 6.45 cm.

Based on the peak frequency we find that $h/L_0=0.30$ (L_0 being the deep water wave length) at the offshore boundary and this makes the test very demanding for weakly dispersive Boussinesq models. Model I, which incorporates Padé [2,2] dispersion characteristics, is resticted to h/L_0 values less than approximately 0.5 and beyond this limit errors in the linear dispersion relation will exceed 5% (see Madsen et al., 1991). Hence an accurate representation of free waves at 2.0 Hz (two times

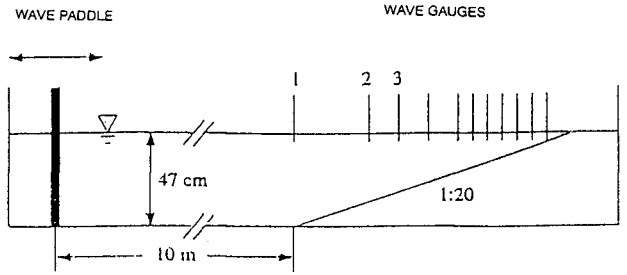

Figure 5 Sketch of physical wave flume (Cox et al. (1991).

the peak frequency) requires the water depth to be less than 0.25 m. For this reason model I does not cover the full domain of the experimental flume, but it is started at station WG4 in a depth of 0.25 m. Model II, on the other hand, incorporates Padé [4,4] dispersion characteristics, which are accurate for h/L_0 as high as 1.0. Hence this model is started at WG1 at a depth of 0.47 m. In both cases the following procedure is used to obtain the incoming wave conditions: First, the measured surface elevation at WG4 (model I) and WG1 (model II) is analysed by FFT. Second, a bandpass filter is applied to remove the energy on frequencies lower than f=0.4 Hz, and higher than f=3.0 Hz. Third, the remaining energy is synthesized back into a flux or a velocity boundary condition by the use of a second order pertubation theory corresponding to each of the model equations.

Fig. 6a-c show the measured and computed spatial variations of the significant wave height, the skewness and the asymmetry. For both models the predicted wave heights are in fairly good agreement with the measurements. From Fig. 6b we notice that the skewness computed by model I is seen to be significantly underestimated everywhere in the flume, while model II picks up the correct variation of this quantity. The skewness is a measure of the nonlinearity in the wave profile and we notice that the results obtained in Fig. 6b confirm the analysis of the transfer function to second harmonics as shown in Fig. 1. Fig. 6c shows the spatial variation of the measured and computed asymmetry. This quantity, which measures the forward pitching of the wave profiles, is almost zero up to the break point beyond which the value decreases drastically. The results obtained by model II are seen to be in almost perfect agreement with the measurements. This result is remarkable and it confirms that the time-domain surf zone Boussinesq model can provide an accurate prediction of the statistics of the wave shape under the combined influence of triad interactions and wave breaking.

Fig 7 shows the measured and computed energy spectra at three locations (WG7, WG9, WG11). Model II is seen to be in very good agreement with the measurements, while model I tends to underestimate the high frequency tail of the spectrum. As mentioned above, the input spectrum used for model I, did not contain energy for frequencies higher than 3.0 Hz. Hence, whatever is present beyond this frequency limit in more shallow water is generated by triad interactions. It is therefore not surprising that the high frequency tail is underestimated by model I.

3.3 Irregular waves on a barred beach

This case is based on the Delta Flume '93 laboratory experiment (Arcilla et al., 1994) which was conducted on a barred beach (Fig. 8d) using a Pierson-Moskowitz spectrum with peak frequency of 0.122 Hz and a significant wave height of 0.58 m. The procedure described in section 3.2 to obtain the incoming wave conditions is also applied here. Fig. 8a-c shows the computed spatial variation of the significant wave height, skewness and asymmetry for the two Boussinesq models. Again the two models predict almost the same variation of the wave heights while significant differences appear in the measures of the nonlinearity: Model I clearly underpredicts the skewness (as well as the asymmetry) while model II is in very good agreement with the measurements.

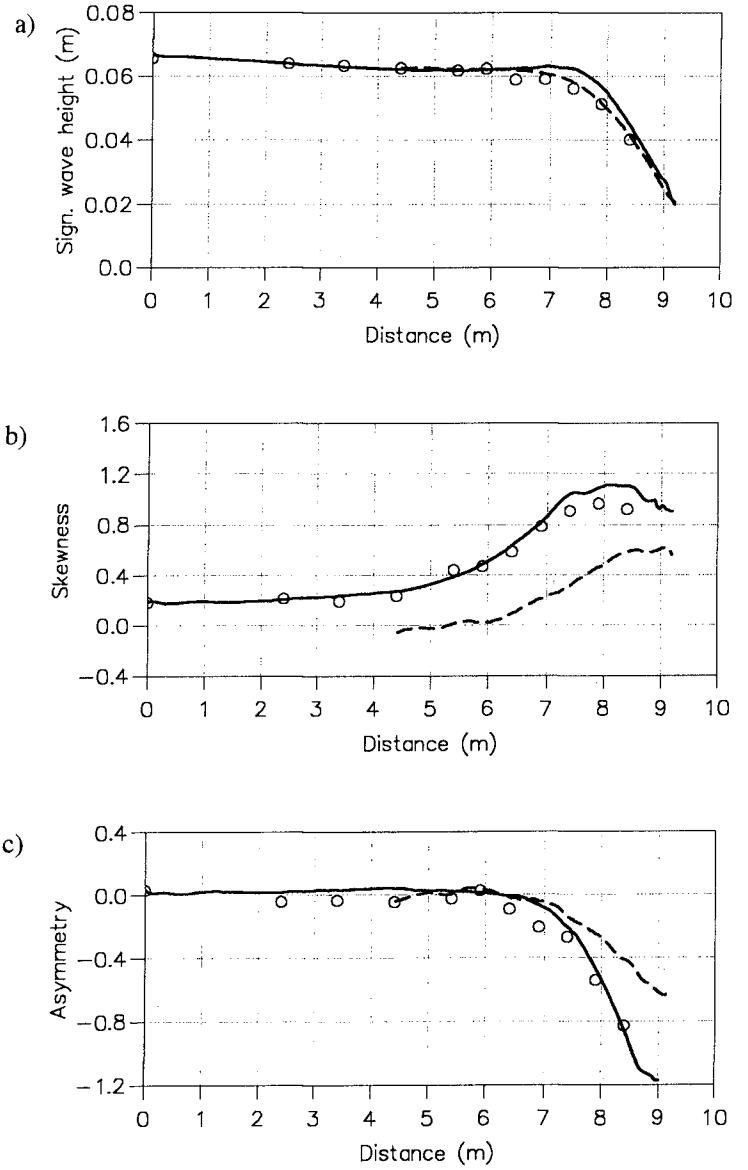

Figure 6 Irregular wave on a plane beach. Spatial variation of (a) the significant wave height, (b) skewness, (c) asymmetry. (- - -) Model I; (——) Model II; (o) Experimental data by Cox et al. (1991).

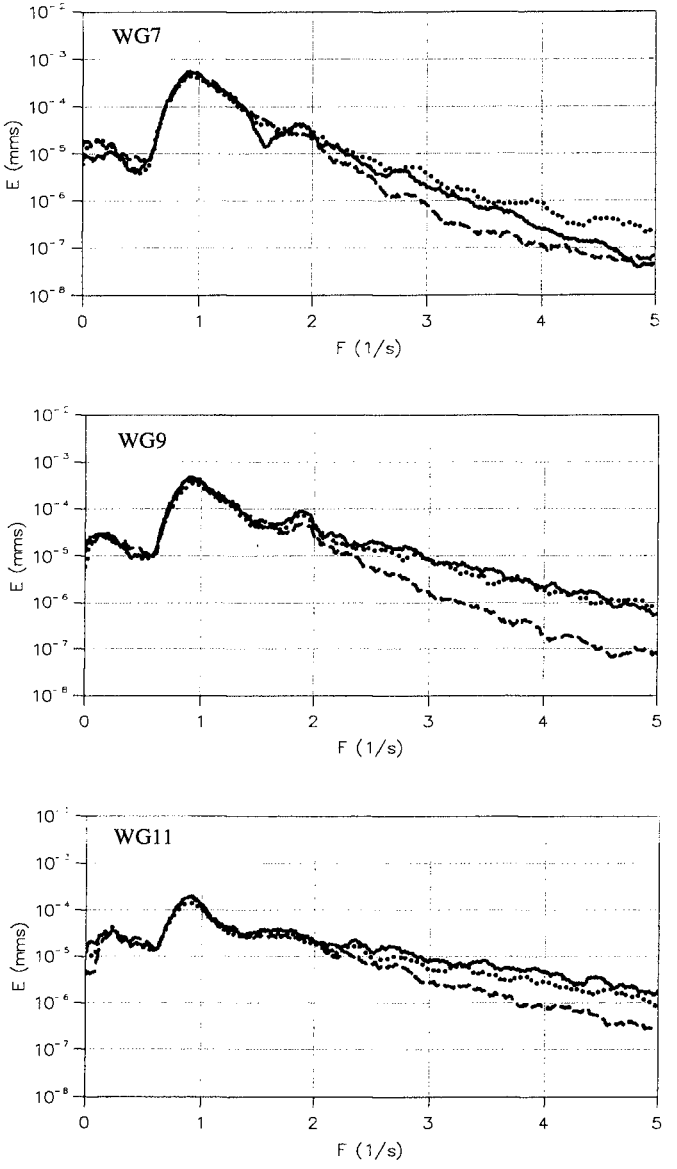

Figure 7 Surface elevation spectra at three locations. (- - -) Model I; (——) Model II; (.....) Experimental data by Cox et al. (1991).

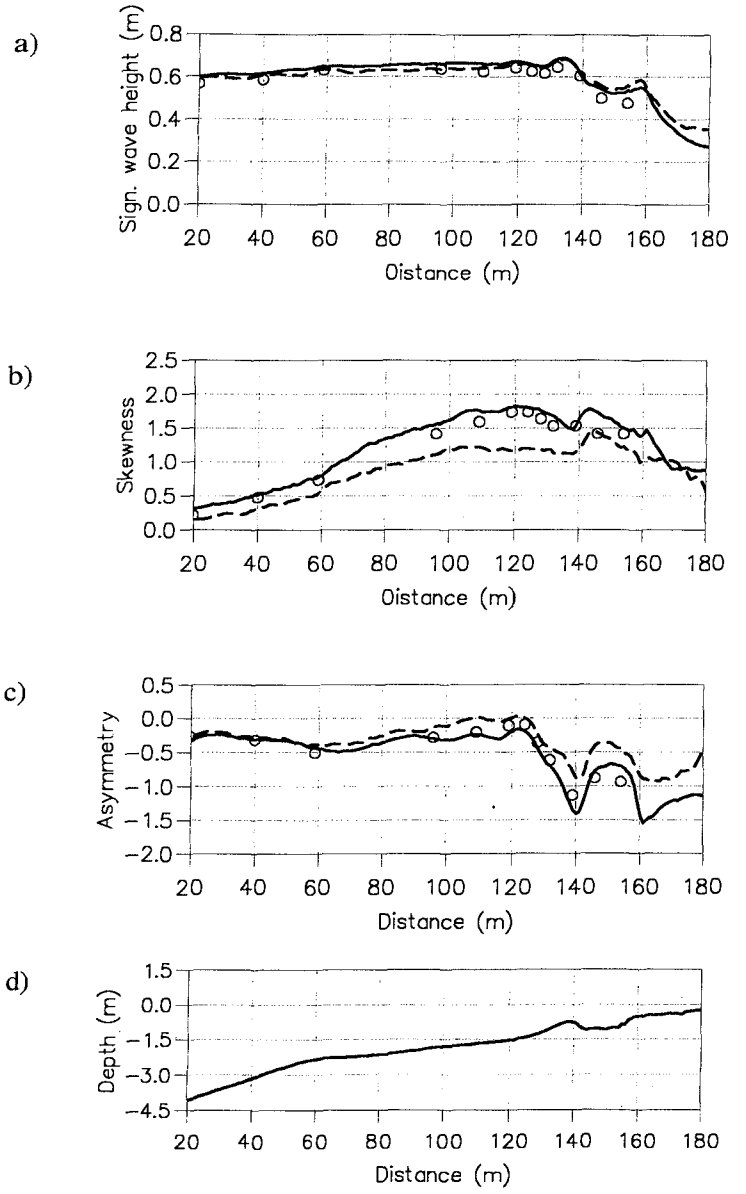

Figure 8 Irregular waves on a barred beach. Spatial variation of (a) the significant wave height, (b) skewness, (c) asymmetry and (d) bathymetry. (- - -) Model I; (——) Model II; (o) Experimental data by Arcilla et al. (1994).

4. Waves in an opposing current

Boussinesq model II is Galilean invariant in contrast to model I, and it provides Padé [4,4] dispersion characteristics with the correct Doppler shift in connection with ambient uniform currents (see e.g. Madsen & Schäffer, 1998a,b). In this work we have applied model II to study the phenomenon of wave breaking in adverse currents. We have focused on the experiments by Sakai et al.(1981) who investigated breaker types and breaker depth indices for a variety of opposing currents, beach slopes and deep water wave stepnesses. The experiments were performed in a 24 m long, 0.36 m wide and 0.80 m deep wave flume as shown in Fig. 9. In this paper we present results for the following cases: A beach slope of s = 1/30, regular waves with wave period of T = 1.2 s, wave heights in the interval between 0.009 m and 0.180 m and the current discharges of q = 0, 0.0169 m^2/s and 0.0297 m^2/s.

Fig. 10 shows the calculated breaker depth index h_B/L_0 as a function of the deep water wave steepness H_0/L_0. Here h_B is the still water depth at the break point, H_0 is the wave height in deep water and L_0 is the deep water wave length. We notice that the breaker depth clearly increases for increasing currents and that the model results are in good agreement with the measurements.

Sakai et al. (1988) presented emperical formulas for breaking conditions of shoaling waves on opposing currents. These were based on the extensive flume experiments by Sakai et al. (1981, 1984) and they give the ratio of the breaker depth, R_h, with and without current and likewise for the breaker height, R_H. Both ratios are given as function of a new parameter γ which accounts for the combined effect of the discharge, the incident wave steepness and the slope of the bed

$$\gamma = q^* s^{1/4} (H_0/L_0)^{-1} \tag{6}$$

where

$$q^* = q g^{-2} T^{-3} \tag{7}$$

In Fig. 11 the calculated values of R_h and R_H are compared with the emperical formulas by Sakai et al. (1988). It is seen that for the relative breaker depth the

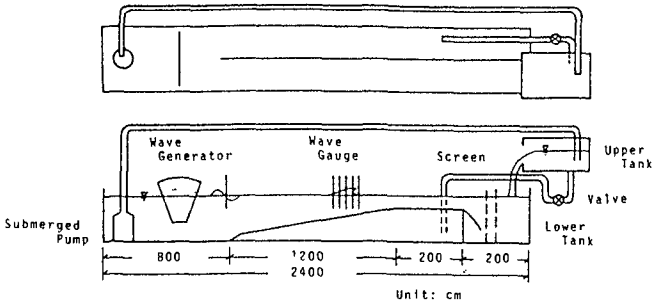

Figure 9 Experiment setup by Sakai et al. (1981).

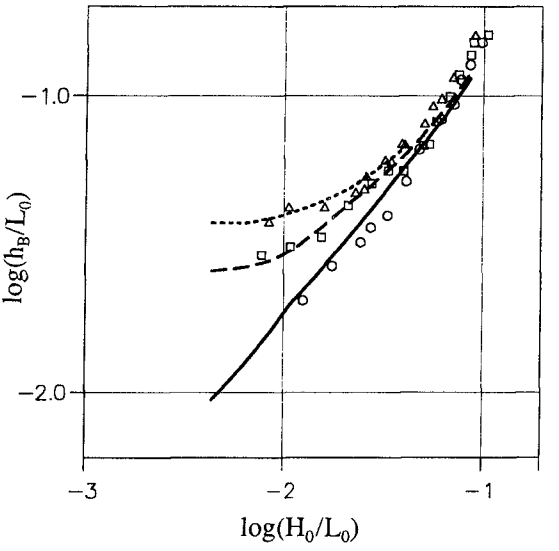

Figure 10 Breaker depth index, h_b/L_0 as funtion of the deep water wave steepness H_0/L_0. Lines show calculations with Model II (——) q=0, (- - -) q=0.0169 m^2/s, (....) q=0.0297 m^2/s; Markers show measurements by Sakai et al. (1981), (o) q=0, (□) q=0.0169 m^2/s, (Δ) q=0.0297 m^2/s.

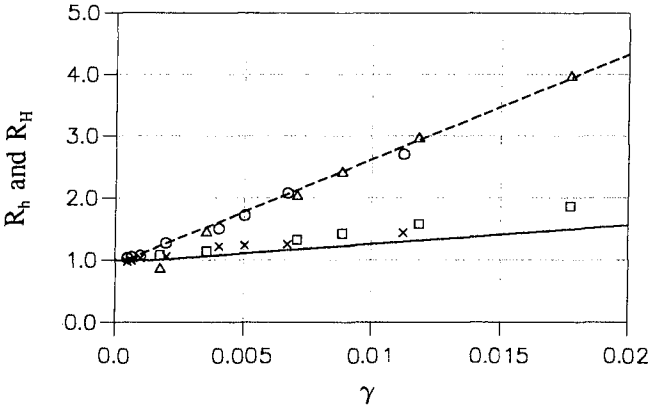

Figure 11 Relative breaker depth and relative breaker height as function of the parameter γ. Lines show formulas by Sakai et al. (1988), (- - -) R_h and (——) R_H; Markers show calculation with Model II, (○) R_h for q=0.0169 m^2/s, (Δ) R_h for q=0.0297 m^2/s; (×) R_H for q=0.0169 m^2/s and (□) R_H for q=0.0297 m^2/s.

agreement with measurements are quite good, while the relative breaker height seems to be overestimated.

Acknowledgements

This research was funded by the Danish National Research Foundation and their support is greatly appreciated. Many thanks to Peter Kjeldsen who contributed to the work concerning waves in an opposing current.

REFERENCES

Arcilla, A.S., Roelvink, J.A., Connor, B.A., Reiners, A. and Jimenez, J.A. (1994), The Delta flume '93 experiment", Proc. Coastal Dynamics Conf., UPC, Barcelona, pp. 488-502.

Cox, D.T., Mase, H. and Sakai,T. (1991), An experiment on the effect of fluid acceleration on seabed stability. Report no. 91-HY-01, Kyoto University, Japan.

Madsen, P.A. and Schäffer, H.A. (1998a). Higher order Boussinesq-type equations for surface gravity waves - Derivation and analysis. Phil. Trans. Roy. Soc., Series A, London, Vol 356,1-59.

Madsen, P.A. and Schäffer, H.A. (1998b), A Review of Boussinesq-type equations for surface gravity waves. In Advances in Coastal and Ocean Engineering, Vol 5., World Scientific.

Madsen, P.A., Sørensen , O.R. and Schäffer H.A. (1997a), Surf zone dynamics by a Boussinesq type model. Part I. Model description and cross-shore motion of regular waves, Coastal Eng., 32, 255-287.

Madsen, P.A., Sørensen , O.R. and Schäffer H.A. (1997b), Surf zone dynamics by a Boussinesq type model. Part II. Surf beat and swash oscillations for wave groups and irregular waves, Coastal Eng., 32, 289-319.

Madsen, P.A., Banijamali, B., Schäffer, H.A. and Sørensen, O.R. (1996), Higher Order Boussinesq Type Equations with Improved Dispersion and Nonlinearity, Proc. 25nd Int. Conf. Coastal Eng., Florida, USA, pp. 95-108.

Madsen, P.A., and Sørensen, O.R (1992), A new form of the Boussinesq equations with improved linear dispersion characteristics. Part II. Coastal Eng., Vol 18, 183-204.

Sakai, S. Hirayama, K. and Saeki, H. (1988), A new parameter for wave breaking with opposing current on a sloping sea bed, Proc. 21st Conf. Coastal Eng., Spain, pp. 1035-1044.

Sakai S. and Saeki H., Effects of opposing current on wave transformation on sloping sea bed, Proc. 19th Conf. Coastal Eng., Texas, USA, pp. 1132-1148.

Sakai S., Otsuka, Saeki H. and Ozaki A. (1981), Interaction between finite amplitude waves and opposing currents on sloping sea bed, Proc. International Symposium on Hydrodynamics, Norwegain Institute of Technology, Tronheim, Norway.

Schäffer, H.A., Madsen, P.A. and Deigaard, R. (1993), A Boussinesq model for waves breaking in shallow water, Coastal Eng., 20, 185-202.

Sørensen , O.R., Schäffer H.A. and Madsen, P.A. (1998), Surf zone dynamics by a Boussinesq type model. Part III. Wave induced horizontal nearshore circulations, Coastal Eng., 33, 155-176.

Ting, F.C.K and Kirby, J.T. (1994), Observation of undertow and turbulence in a laboratory surf zone. Coastal Eng., 24, 51-80.